International Conference on Space Optics—ICSO 2022

Dubrovnik, Croatia

3–7 October 2022

Edited by Kyriaki Minoglou, Nikos Karafolas, and Bruno Cugny,

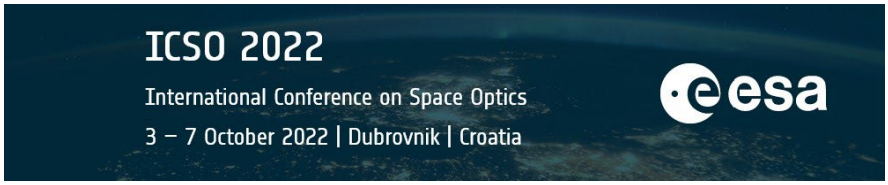

A compressive sensing with photonic crystals enabled spectrometer for trace gas observation

International Conference on Space Optics — ICSO 2022, edited by Kyriaki Minoglou, Nikos Karafolas, Bruno Cugny, Proc. of SPIE Vol. 12777, 127776Y · © 2023 ESA and CNES · 0277-786X · doi: 10.1117/12.2691361

A compressive sensing with photonic crystals enabled spectrometer for trace gas observation

M.E. Siemons[a], M. Hagenaar[a,b], A.J.L. Adam[b], R. Kohlhaas[a,b];
[a] SRON Netherlands Institute for Space Research, Niels Bohrweg 4, 2333 CA Leiden, the Netherlands; [b] Delft University of Technology, Faculty of Applied Sciences, Dep. of Imaging Science and Technology, Optics Research Group, Lorentzweg 1, 2628 CJ Delft, the Netherlands

ABSTRACT

Recently a spectrometer concept has been invented which uses compressive sensing in combination with photonic crystal filters. Here we present an adaption of this concept in push-broom configuration for earth observation. This implementation allows for a compact design, while maintaining a high spatial resolution and high signal-to-noise ratio compared to other traditional implementations. The photonic crystals have a unique transmission profile and act as a spectral filter, which allows for the computational reconstruction of the input spectrum with a limited number of filters. We show, using simulations, that our approach is able to reconstruct input radiance spectra with high accuracy and assess the performance for different number of filter sets. We furthermore show proof-of-principle measurements of the transmission profile of a manufactured photonic crystal. Future research will focus on the effect of noise on the reconstruction algorithm as well as further filter set optimization by combining the filter selection process with trace gas concentration retrieval.

Keywords: Spectrometer, computation inversion, compressive sensing, photonic crystals, trace gases, earth observation

1. INTRODUCTION

The need for the monitoring of greenhouse gas emission sources motivates the development of earth observation systems with a higher spatial and temporal resolution. Here for example hybrid solutions are an option, which combine low field-of-view, high spatial resolution instruments with large field-of-view, low spatial resolution instruments, as recently demonstrated in the measurement of methane emissions from landfills using TROPOMI and GHGsat satellite data [1]. Alternatively, complete distributed systems with many satellites could be considered. This would require small, low-weight optical imaging spectrometers. Conventional grating spectrometers have intrinsic physical limits on the system size due to the need of large free-space optical path length for the separation of wavelengths. Other solutions, as for example static Fourier-transform spectrometers as developed with NanoCarb [2], suffer less from such limitations. Recently, a spectrometer concept was invented [3] which uses an array of photonic crystal filters with quasi-random spectral transmission functions together with computational inversion (for example compressive sensing) to reconstruct the input spectrum. In this work we investigate if this concept could be transferred to earth observation and choose as a first application example the detection of methane in a spectral range of 1625 nm to 1670 nm.

1.1 Instrument concept

The instrument concept is centered around the computational spectrum inversion using compressive sensing. Compressive sensing is a signal processing technique for efficiently acquiring and reconstructing a signal. It can find a solution to an underdetermined linear system where the number of measurement (M) is smaller than the sampling points (N) of the to be determined signal [4]. In general, this is not possible as stated by the Nyquist sampling theorem. However, it can be achieved if the signal is sufficiently sparse in some base or representation. The prior knowledge of this sparsity allows reconstruction algorithms to find solutions to the underdetermined linear systems which approximate the underlying signal very well. The under sampling enables many types of advantages, such as reduced data flow, improved signal-to-noise ratio (SNR) or increased data acquisition speed. For these reasons compressive sensing is currently used in many applications, such as imaging, pattern recognition and video processing [4]. Because absorption bands of trace gases are highly periodic, radiance spectra of the earth can be effectively described in a Fourier base to create a sparse signal. Using compressive sensing it is possible to therefore reconstruct a detailed spectrum with fewer measurements ($M < N$). Such an approach would result in a high SNR compared to a linear gradient filter, allowing an uncompromised compact instrument with high resolution and high spectral accuracy.

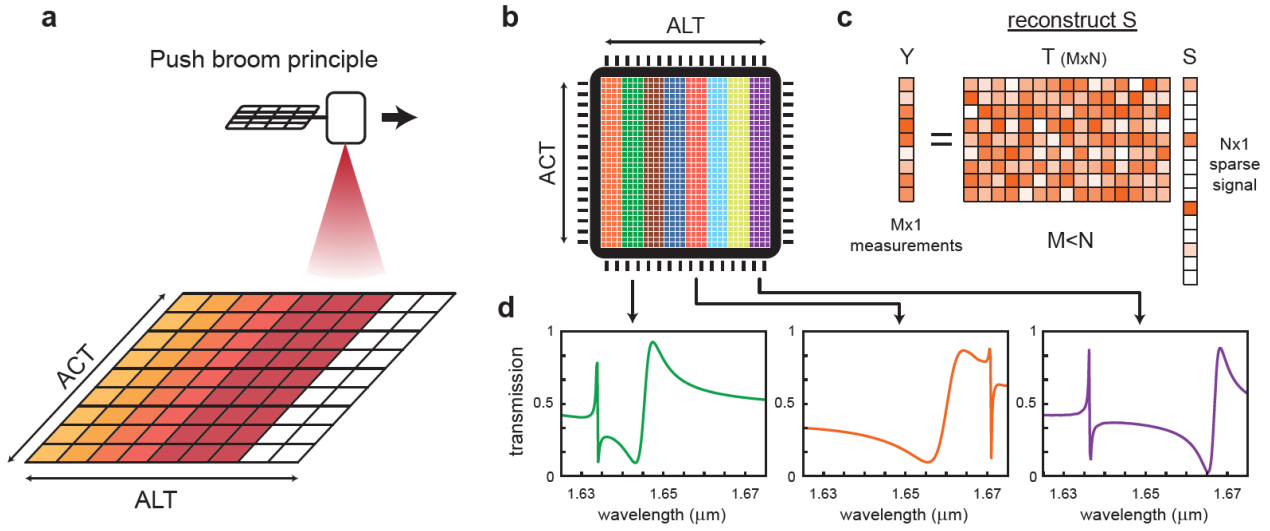

Figure 1. Instrument concept. a) The instrument uses the push broom principle the measure the intensity transmitted by each filter. b) The spectral filters cover the pixels of the focal plane array in a column wise fashion, covering multiple pixels. c) Principle of compressive sensing. Here a solution to signal S (Nx1) is found with Y (Mx1) measurements. D) Each spectral filter has a unique spectral transmission profile.

Here we propose the following instrument concept, which has similarities with a linear gradient filter spectrometer, but making use of compressive sensing, see Figure 1. The instrument orbits the earth and consists of an earth observing telescope. A wafer with a dielectric material (in our case a glass wafer with a 400 nm thin Si-film) is bonded on the sensor. It contains 2D photonic crystals in a column wise arrangement in the across-track (ACT) direction. These photonic crystals consist of sub-wavelength features etched in the Si-film and have unique spectral transmission profiles. These transmission profiles arise from resonances in the Si-film and depend on the thickness of the film as well as the specific shape and size of the etched structure and the lattice size. By choosing a specific hole shape and lattice size, different spectral transmission profiles can be achieved. Using the push-broom concept, the transmitted intensity for each ground instantaneous field of view pixel can be measured for each spectral filter. This allows a far larger field-of-view in along-track (ALT) direction than with an imaging spectrometer with a slit. As only a limited number of filters is needed to reconstruct the spectrum, the filters can cover multiple pixels of the sensor. Imaging in ACT direction follows the conventional push-broom concept. From the transmission measurements in ALT direction of the same ground scene an input spectrum can be reconstructed.

1.2 Conceptual advantages and disadvantages

The instrument concept presented here features several advantages over existing implementations. It is smaller than a grating spectrometer since no additional free space optical path length is needed for wavelength separation. Moreover, different spectral ranges can be combined on one detector (for example the O2A band and methane band, or several relevant methane spectral ranges). The concept is similar to the linear gradient filter concept, but it features a higher spectral bandwidth per filter and therefore has a much higher SNR. This is in turn amplified as the spectrum reconstruction using compressive sensing potentially allows to decrease the number of required filters, which further increases the SNR. However, we expect that the performance of such an instrument might suffer in fast changing scenes and in addition will require thorough calibration.

2. METHODS

2.1 Computational spectrum reconstruction

The measured intensity I_m of filter m can be described as

$$I_m = \int_\lambda S^{in}(\lambda) T_m(\lambda) D(\lambda) d\lambda \quad (1)$$

where S^{in} (λ) is the input signal, D(λ) the detector response and T_m (λ) the transmission function of filter m. Alternatively, with λ discretized and the detector response neglected, eq. 1 can be reformulated as a system of equations and stated as a compressive sensing problem

$$\begin{bmatrix} I_1 \\ \vdots \\ I_M \end{bmatrix} = \begin{bmatrix} T_{11} & \cdots & T_{N1} \\ \vdots & \ddots & \vdots \\ T_{M1} & \cdots & T_{NM} \end{bmatrix} \begin{bmatrix} S_1 \\ \vdots \\ S_N \end{bmatrix} \quad (2)$$

where M is the total numbers of filters with $N > M$. Here T denotes a matrix containing the transmissions of the spectral filters. Each row of T corresponds to the spectral transmission of one filter. Because $N > M$, eq. 2 does not have a unique solution in general. A unique solution to the problem of eq. 2 can still be found by minimizing the L1-norm of the reconstructed signal in a sparse base, here assumed to be Fourier space

$$\min_{\tilde{S}} \left|\tilde{S}\right|_1 \quad \text{subject to } I = T\phi^{-1}\tilde{S} \quad (3)$$

where ϕ^{-1} is the inverse Fourier transform matrix and $\tilde{S}$ the Fourier transformed signal. However, finding this solution in practice is computationally intense. Alternatively, the problem can be regularized as follows

$$\min_{\alpha,\tilde{S}} \left|\mathrm{I} - \mathrm{T}\phi^{-1}\tilde{S}\right|_2 + \alpha\left|\tilde{S}\right|_1 \quad \text{subject to } I = T\phi^{-1}\tilde{S} \quad (4)$$

where α denotes the regularization factor. Also called penalty coefficient, α in eq. 4 can be interpreted as the sparsity constraint on the solution. For the limit where α approaches zero, the residue term dominates, and the problem effectively reduces to an energy minimization problem. In the limit where α approaches infinite, the length term dominates and solutions for S including many non-zeros are penalized. A balance can be found where a specific sparsity can be retrieved for a specific α [5]. Here we use the LASSO algorithm, which is a standard optimization algorithm for compressive sensing, to find a solution of eq. 4. Alternatively, Ordinary Least Squares (OLS) can be used in combination with gradient decent to find a solution with α = 0.

2.2 Photonic crystal based spectral filters

The compressive sensing algorithm can reconstruct the unknown signal as best as possible if the transmission profiles of the photonic crystals are highly uncorrelated [6]. To obtain such uncorrelated set of filters we first created a library of photonics crystals in a wide variety of shapes: squares, circles, octagons, and two types of crosses in a range of different sizes (w) and lattice constants (Lc). See Figure 2. We used finite-difference time-domain (FDTD) electromagnetic simulations in Lumerical (version 3.8, 2022) to compute the spectral transmissions. The relevant simulation settings used are: pulse length of 15 ps and a mesh accuracy of 2 (mesh size depended on refractive index of the material, 6 spatial samplings per wavelength). We varied the lattice constant between [600,2000] nm with steps of 20 nm and the width of the structures ranging from 0.25Lc to 0.65Lc in 5 steps. After some initial filtering to remove uninteresting configurations we ended up with a library of around 1300 filters.

After the library generation a set of filters with a low amount of correlation must be obtained. The three steps of this filter selection procedure are as follows. First, 700 filters were iteratively removed using singular-value decomposition (SVD). For this the row and column wise correlations are computed to perform the singular value decomposition. The filter which

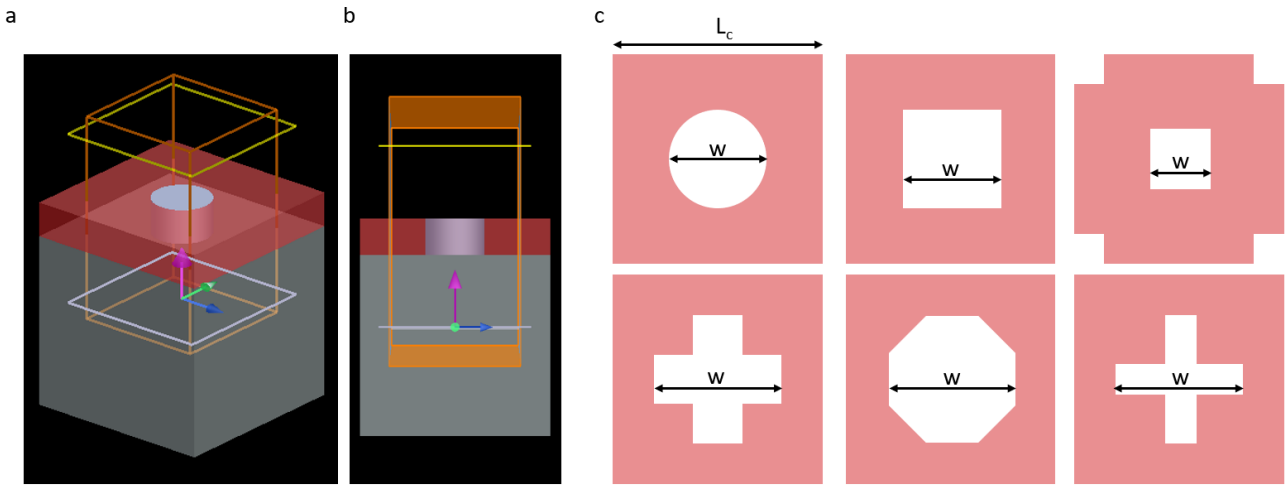

Figure 2. Illustration of the FDTD simulation and the investigated shapes. A&B) 3D rendering of the simulation domain. Grey: SiO2 substrate; red: Si-film; white: etched structure; orange: simulation domain incl Perfectly matched boundary (PML) layer.

best resembles the most common mode is removed and the process if repeated until 600 filters were left. In the second step of the filter selection the pairwise correlations of the remaining filters are ranked and the filter of the pair with the highest correlation is removed. The filter with the least amount of correlation with the rest of the filter set is kept, the other filter is discarded. This process is repeated until the desired number of filters is achieved.

The acquired filter set is now highly uncorrelated, but there is a chance that uncorrelated filters have been removed in step 1. Therefore, the last step of obtaining an uncorrelated filter set involves re-introducing discarded, but potentially better filters. Potential candidate filters are identified by comparing the correlations between the current set of filters and the removed filters. If a removed filter has a smaller correlation with respect to all filters in the current set, it is replaced with one of the two filters that has the largest correlation. The choice of filter between these two depends on their respective L2-norm of the overall correlation with the complete set.

Using this procedure, we obtained several sets of filters with a different total number of filters ranging from 200 to 40. A reduced amount of filters is in principle favorable because this increases the SNR as each filter can cover more pixels. However, less filters might decrease the spectral reconstruction quality due to a lower amount of input information.

2.3 Input methane radiance spectrum

To test the signal reconstruction of the compressive sensing algorithm an input spectrum is required which act as ground truth signal for the signal reconstruction algorithm. We simulated an earth radiance spectrum using a non-scattering radiative transfer model for the atmosphere, assuming Lambertian reflectance at the surface of the earth. The relevant molecule absorption bands are obtained from the HITRAN database [7] and we assumed a methane concentration of 2000 ppb. The data set is simulated with a non-linear sampling of 0.005 nm in a spectral range of 1625 nm to 1670 nm for an albedo of 0.15, sun zenith angle of 70 degrees and nadir observation. Here we focus on the radiance between 1625 nm and 1670 nm where periodic methane absorption bands present. This spectrum act as the ground truth signal and allows the quantification of the reconstruction error of the compressive sensing algorithm.

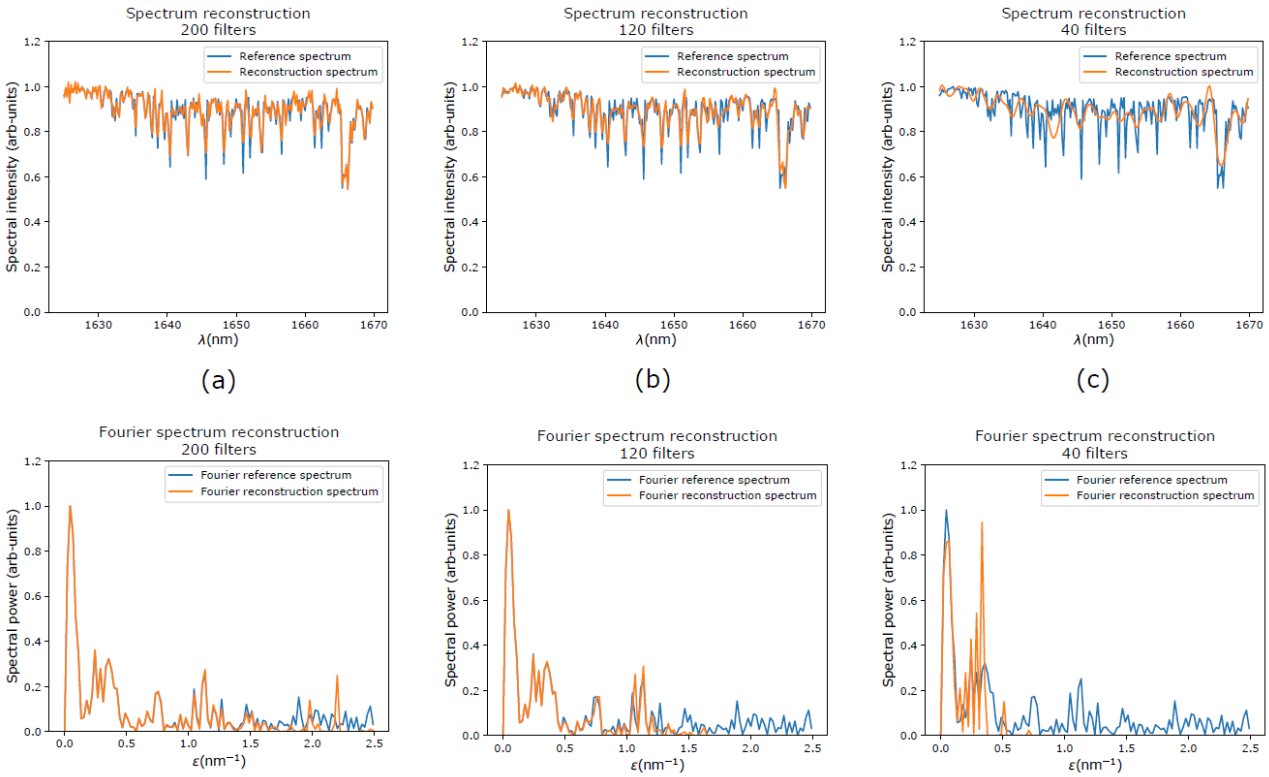

Figure 3. Comparison between ground truth and reconstructed spectrum for different sized filer sets A-C) reconstruction with 200 (A), 120 (B) and 40 (C) filters used. D-F) Fourier transform of the ground truth signal and reconstructed signal for (A-C).

3. RESULTS

We compared the ground truth input signal with the reconstructed signal obtained with different number of filters as shown in Figure 5. The reconstructed signal in the case of 200 filters matches well with the ground truth input spectrum. As expected, the difference between these increases when using less filters. The signal reconstruction in Fourier space (Figure 3d-f) shows that the high spatial frequency components are not faithfully reconstructed. In the case of 200 filters, this appears to occur around spatial frequencies of 1.5 nm^{-1}, while filter sets with a number of 120 and 40 are roughly able to reconstruct spatial frequencies up to 1 nm^{-1} and 0.25 nm^{-1} respectively. This likely occurs because the photonic crystals do not have enough sharp spectral features, which is needed to reconstruct the high spatial frequency information. Nonetheless, such spectral information is in general not required to retrieve trace gas concentrations. For instance, the TANGO concept (Twin Anthropogenic Greenhouse gas Observers [8]), designed to measure methane concentration, features an Instrument Response Spectral Response Function (ISRF) with a size 0.45 nm. The measured spectrum with a standard spectrometer can be described over the convolution of the input signal with the ISRF, which limits the spectral resolution.

To compare our compressive sensing approach with the results obtained using a standard spectrometer we convolved the simulated input spectrum and the reconstructed spectrum with a 0.45 nm sized ISRF and juxtaposed them. These results, shown in Figure 5, show an excellent match between reconstructed and ground truth signal, especially when using a filter set of size 200. Again, high spatial frequency information is lost when using less filters, but not as severe as in the unconvolved case. Lastly, we compared the relative error as function number of used filters for both the unconvolved and convolved case, shown in Figure 4, both using the LASSO algorithm as well as with ordinary least squares (OLS). These results show that is possible to reconstruct a signal with relative errors as low as 4% (unconvolved) and 1.5% (convolved) and show a clear tradeoff between the amount of filter used and the reconstruction accuracy. We note that this is the case without noise present. Using less filters increases the SNR as each filter can cover more pixels of the sensor but lowers the reconstruction accuracy. Therefore, these simulation results show that this approach has the potential to perform spectrometry for earth observation.

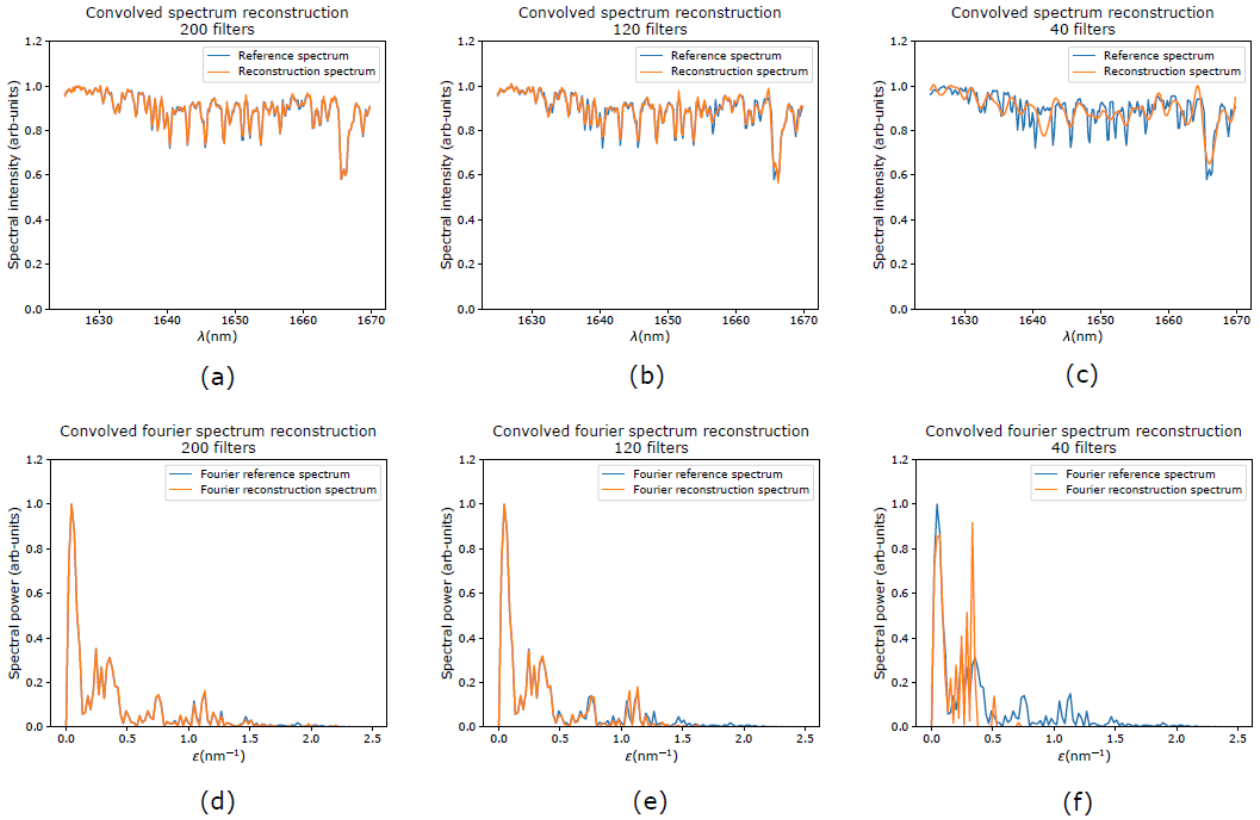

Figure 5. Comparison between convolved ground truth and reconstructed spectrum for different number of filer sets A-C) reconstruction with 200 (A), 120 (B) and 40 (C) filters used. D-F) Fourier transform of the convolved ground truth signal and reconstructed signal for (A-C).

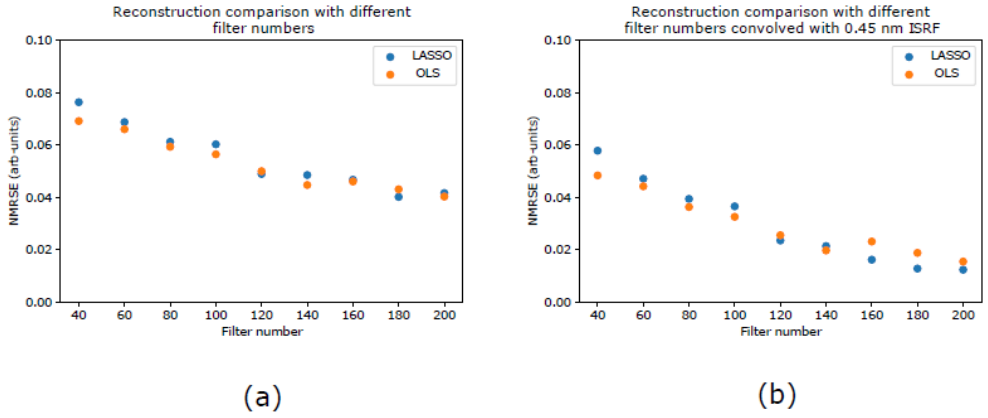

Figure 4. Relative reconstruction error as function of filter set number of the reconstructed spectra in the case with an unconvolved (A) and convolved ground truth spectrum.

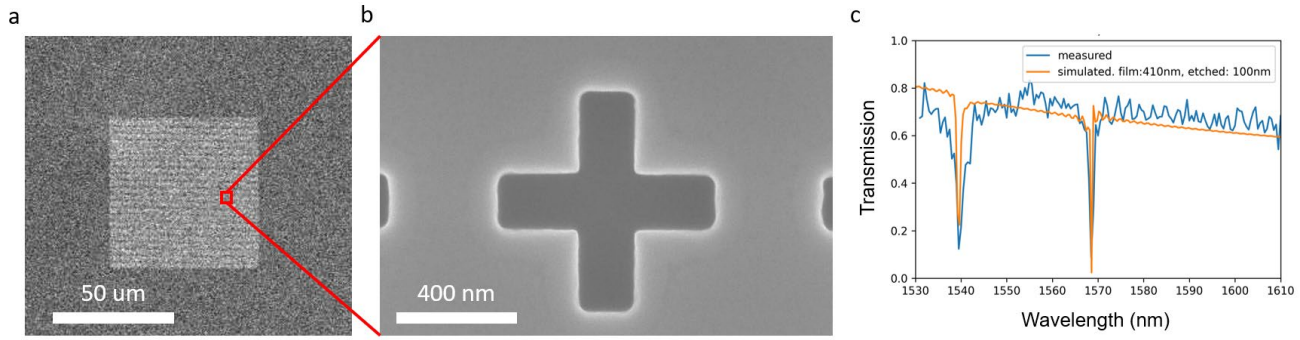

Figure 6. A-B) SEM images of the manufactured photonic crystal. C) Measured transmission as function of wavelength compared to the simulated transmission.

3.1 Experimentally measured filter transmission

To demonstrate the experimentally viability we have manufactured a test proof-of-principle spectral filter using e-beam lithography and measured the spectral transmission of the photonic crystal, see Figure 4. The spectral transmission was measured using a setup which contained a tunable laser in the range of 1530-1610 nm (Newport, custom version of TLB-6730-P). The laser emission was collimated using a reflective fiber collimator (Thorlabs, RC04FC-P01) and directed to the wafer. The small etched region was then imaged by a 4X imaging relay onto a InGaAs sensor (Xenics, Xena640). Etalon effects of the wafer were removed by a fitting algorithm.

The measured transmission, shown in Figure 6c is in good correspondence with the simulated transmission, thereby validating our filter simulation framework. However, the spectral feature around 1540 nm is not as sharp as the spectral feature at 1568 nm. There also appears a slight overall difference in transmission. Both these differences between simulation and measured transmission are attributed to manufacturing precision and tolerances, such as the precise thickness of the Si-film and defects in the etching processes. These results show that it is possible to create very sharp spectral features, but also indicate that the lithography protocol needs to be further optimized to achieve a consistent performance of these photonic crystals.

4. CONCLUSION AND OUTLOOK

In summary, we presented a novel spectrometer concept which uses photonic crystals in combination with compressive sensing. A photonic crystal array with distinct spectral transmission profiles is used to reconstruct radiance spectra from the earth, which can be used for trace gas measurements. This concept allows for the combination of a compact instrument with a high SNR and spatial resolution. Using FDTD simulation we created a library of photonic crystal filters and performed several selection steps to create a sets of uncorrelated transmission profiles. Using these filter sets, we applied a computational inversion with compressive sensing to reconstruct a simulated radiance spectrum. The reconstructed spectra correspond well to the input spectrum for low spatial frequencies but fail to reconstruct sharp spectral features. More research is needed to analyze the impact of this for trace gas concentration retrieval, as well as the impact of noise. Lastly, we showed preliminary experimental results on the transmission profile of a manufactured filter and compared this to the simulated transmission profile. These appear to match, indicating that these FDTD simulation give physical results, but also hints towards further improvements in the lithography protocol.

ACKNOWLEDGEMENTS

This work was supported by a system study grant from the Open Space Innovation Platform (OSIP) of the European Space Agency (ESA). We thank Carel Herkens from TU Delft for the manufacturing of the photonic crystals, Paul Tol from SRON for input on the methane spectra and René Berlich from ESA for general discussion and input.

CONTRIBUTIONS

RK conceived research. MH performed the simulations and MS performed the experimental measurements. RK & AA supervised the project. RK and MS wrote the article with input from AA.

REFERENCES

[1] J. D. Maasakkers, D. J. Varon, A. Elfarsdóttir, J. McKeever, D. Jervis, G. Mahapatra, S. Pandey, A. Lorente, T. Borsdorff, L. R. Foorthuis, B. J. Schuit, P. Tol, T. A. van Kempen, R. van Hees and I. Aben, "Using satellites to uncover large methane emissions from landfills," *Science Advances,* vol. 8, August 2022.

[2] S. Gousset, N. Guérineau, L. Croizé, E. L. Coarer, T. Laveille and Y. Ferrec, "NANOCARB-21: a miniature Fourier-transform spectro-imaging concept for a daily monitoring of greenhouse gas concentration on the Earth surface," in *International Conference on Space Optics — ICSO 2016*, 2017.

[3] Z. Wang, S. Yi, A. Chen, M. Zhou, T. S. Luk, A. James, J. Nogan, W. Ross, G. Joe, A. Shahsafi, K. X. Wang, M. A. Kats and Z. Yu, "Single-shot on-chip spectral sensors based on photonic crystal slabs," *Nature Communications,* vol. 10, March 2019.

[4] M. Rani, S. B. Dhok and R. B. Deshmukh, "A Systematic Review of Compressive Sensing: Concepts, Implementations and Applications," *IEEE Access,* vol. 6, p. 4875–4894, 2018.

[5] T. Hastie, R. Tibshirani and J. Friedman, The Elements of Statistical Learning Data Mining, Inference, and Prediction, Second Edition, Springer, p. 768.

[6] M. Fornasier, Ed., "Compressive Sensing and Structured Random Matrices," in *Theoretical Foundations and Numerical Methods for Sparse Recovery*, DE GRUYTER, 2010.

[7] L. S. Rothman, "History of the HITRAN Database," *Nature Reviews Physics,* vol. 3, p. 302–304, April 2021.

[8] J. Landgraf, S. Rusli, R. Cooney, P. Veefkind, T. Vemmix, Z. de Groot, A. Bell, J. Day, A. Leemhuis and B. Sierk, "The TANGO mission: A satellite tandem to measure major sources of anthropogenic greenhouse gas emissions," March 2020.